Observational Study of Nisarg Cyclone Winds using Phased Array Doppler Sodar at Atigre, Kolhapur, India

Rani P. Pawar
Center for Space and Atmospheric Science, Sanjay Ghodawat University, Kolhapur
Thiyagesan dharmaraj
Indian Institute of Tropical Meteorology
Dada P. Nade (dada.nade@gmail.com)
Dr Patangrao Kadam Mahavidyalaya, Sangli https://orcid.org/0000-0003-3604-6863
Mahendra N. Patil
Indian Institute of Tropical Meteorology
Omkar M. Patil
NASA Oklahoma Space Grant Consortium: The University of Oklahoma College of Atmospheric and Geographic Sciences
Jeni Victor
Indian Institute of Tropical Meteorology
S. D. Pawar
Indian Institute of Tropical Meteorology

Research Article

Keywords: Phased Array Doppler Sodar, Tropical Cyclone, Atmospheric Boundary Layer, Vertical Turbulence Intensity etc.

Posted Date: November 3rd, 2021

DOI: https://doi.org/10.21203/rs.3.rs-971499/v1

Abstract

One of the most important parameters in meteorology is the mean wind profile in the tropical cyclone boundary layer. The signature of the Nisarg cyclone is reported in the Phased Array Doppler Sound Detection and Ranging (SODAR) data installed at the Center for Space and Atmospheric Science (CSAS), Sanjay Ghodawat University, Kolhapur (16.74° N, 74.37° E; near India's western coast). The vertical profile of wind speed and wind direction measured from the sodar system clearly reveals the signature of Nisarg cyclone during 2- 3 June 2020. Our analysis revealed that, the maximum mean wind speed was 17 m/s on 3rd June 2020 at 10:00 IST. It also shows the change in the wind direction from southwest to southeast on 2nd June 2020 and 3rd June 2020. Daily high-resolution reanalysis in the domain, 0-25°N, 65-110°E, during the period from 31st May-5th June 2020 shown the variation in atmospheric pressure of the Nisarg cyclone from 1000 to 1008 hPa, sea surface tremperature (SST) between 30 and 31°C, outgoing longwave radiation (OLR) varied between 100 and 240 Wm^{-2}, wind speed between 3 and 15 m/s and low values of vertical wind shear (VWS) was observed to the north of the track Nisarg. These findings could aid in better understanding and forecasting in this region. The present results are initial measurements of sodar system.

1 Introduction

Tropical cyclones (TCs) are one of nature's most devastating occurrences and have the potential to cause severe damage over a wide section of the coastline (Asnani et al. **2005**; Pattanayak et al. **2008**). Property losses have significantly risen due to land-falling cyclones. As coastal populations continue to expand, the instability in the wind field of a land dropping cyclone has become evident both horizontally and vertically. As development continues along the cyclone-prone coastlines of large high-rise buildings, an understanding of the features of the vertical wind profile is sorely required. It is necessary to establish a regional weather forecasting system in order to provide early warnings and reduce calamities. As a result, precise forecasting of cyclone track and severity is critical to minimising human deaths and property damage (Reddy et al. **2014**). The mean wind profile in the tropical cyclone boundary layer is vital to understand the overall dynamics of tropical cyclones because it reflects air-sea momentum transfers that are critical in tropical cyclone weather forecasting (Tse et al. **2013**). The intensity of TCs has been particularly high over the Bay of Bengal, south-west India, during the post-monsoon period of October and November. These TCs grows northwestward, towards India's east coast, over the southern and central Bay of Bengal, as well as the Andaman Sea, and frequently receive between 15°N and 18°N, affecting Bangladesh's coast (Kumar et al. **2014**). During the post-monsoon season, there was an increase in the frequency of extremely violent cyclonic storms across the Arabian Sea (Murakami et al. **2017**).

The number of cyclones created over the Bay of Bengal was 3-4 times more than that over the Arabian Sea, according to (Obasi et al. **1997**). Although cyclones are uncommon in the Arabian Sea, it does produce powerful tropical cyclones (Bhatla et al. **2020**). Several research has been conducted to document the reaction of ocean dynamics in the creation of TCs, as well as to comprehend the relevant air-sea interaction processes (Stramma et al. **1986**, Lyulyukin et al. **2015**, Lyulyukin et al. **2017**, Zaitseva

et al. 2018). The wind speed and the differential in moisture content between the air and the saturation mixing ratio at the sea's surface determine how much energy is transferred from the ocean to the atmosphere in the form of moisture (Chinthalu et al. 2018). The tropical cyclone boundary-layer (TCBL) has the least well-observed component of the storm (Jelesnianski et al. 1993). However, the boundary layer is responsible for cyclone communication with ocean by receiving heat and moisture, and transmitting momentum in the form of oceanic current and waves (Giammanco et al. 2012).

The Sound Detection and Ranging (Sodar), a remote sensing instrument is commonly used to study the atmospheric boundary layer (ABL) and also for regional scale observation of wind turbulence. The transfer and exchange of energy, mass, momentum, and moisture from the lower to the upper layers is governed by boundary layer dynamics. Sodar is suitable to study the lower part of the ABL (Kumar et al, 2011, Kallistratova et al. 2004). In addition to Sodar measurements, other measurements will be helped to visualize three dimensional structure of wind profile. Because terrain roughness and complexity influence the mean wind profile in the approaching direction, it is expected to change under the influence of the sea fetch (Cheynet et al. 2020).

A series of 11 sensitivity experiments were conducted on various physical parameterization schemes of the Weather Research Forecast (WRF-ARW core) model to predict the track and intensity of tropical cyclone Nargis, which formed over the Bay of Bengal and hit Myanmar on May 2, 2008, causing widespread human and economic losses (Raju et al. 2011). Using archival tropical storm track data from the Joint Typhoon Warning Center, a rigorous analysis was undertaken to generate the most likely (synthetic) cyclone track (JTWC) from Sahoo et al. 2017. They found that post-monsoon cyclones occur more frequently than pre-monsoon cyclones. While plotting the route of tropical storms, it is also observed that the path of tropical cyclones abruptly alters during their active life span. According to historical statistics, the main cyclone seasons in the South Indian Ocean are May-July and September-December, with substantial storm occurrences in April and August (Nair et al. 2018). From 2014 to 2018, (Hendricks et al. 2019) published a summary of scientific advances on tropical cyclone intensity change. Improved understanding of the role of vertical wind shear (VWS) and its impact on convection, surface fluxes, ocean eddies, dry/dusty air intrusions, eyewall replacement cycles (ERCs), spiral rainband dynamics, eyewall instability and inner-core mixing, and the mechanisms by which TCs intensify have all resulted from research on intensity change.

The present study attempts to investigate the characteristics of wind during the cyclonic storm Nisarga. A short description of the measuring equipment, Sodar, is given in the second section of this paper. This study presents data of wind speed and direction in the atmospheric boundary layer during the Nisarg cyclone that occurred over the Arabian Sea. We use continuous wind measurements located at a low-latitude station of Atigre, Kolhapur (16.69° N, 74.24° E) which described in detail in the experimental details and data section.

2 Observational Site, Experimental Details And Data Description

The observational site is situated in the outskirt of Kolhapur at Atigre (16.74° N, 74.37° E, 604 AMSL) in the campus of the Sanjay Ghodawat University (SGU), in western Maharashtra State, India. There are hills as high as 600 meter AMSL in the north of the experimental site, and a large agricultural area of sugar cane farms is situated in the southern portion. The eastern side of the experimental site is occupied by the industrial sectors, while the Kolhapur is located on the west side. The details of the observational site has given in (Nade et al. **2020**). The experimental design of the Sodar with enclosure at the observational site is shown in figure 1. The results of wind speed and direction are compared to Automatic Weather Station (AWS) observational data for validation.

The wind measurements by Phased Array Doppler Sodar during the passage of Nisarga Cyclone i.e. from 31st May 2020 to 5th June 2020 were selected and processed. The measurements were carried out using a Sodar with a frequency range of 1800-2500 Hz and a 100 W acoustic power (output). The Doppler sodar phased array system includes 8 × 8 array antenna components. In the height range of 40-980 m beams slanted from the zenith in the east and north directions, the three components of wind speeds along X, Y, and direction, as well as other dispersion parameters (power, signal-to-noise ratio, etc.) have been determined. The wind speed and direction derived from sodar are accurate to within 0.5 m/s and 5°, respectively. The experimental specifications of the sodar used for this study are given in Table 1.

Table 1
Sodar experimental specifications

Parameter	Specifications
No. of elements	64 (8x8)
Antennas/ Radial Components	a1, a2, a3, a4 and a5 with 64 loudspeakers
Vector Components	u- West-East Wind component v- South-North Wind component w- Vertical Wind component
Transmit Frequency	1500 to 4000 Hz (adjustable)
Range	1.5 to 2 km (adjustable)
Angle of antenna	10 to 30 degree (adjustable)
Pulse width	Programmable
Pulse repetition frequency	Programmable
Range Resolution	User defined
Parameters Studied	Wind velocity, Wind direction, Temperature Structure parameter, Radial component, Vectorial component, wind-shearing velocity and direction etc.

For the period 31st May to 5th June 2020, ECMWF's ERA5 reanalysis of several parameters such as pressure, daily SST, winds, Outgoing Longwave Radiation (OLR), and Vertical Wind Shear (VWS) daily data with a resolution of 1°x1° is shown. In the range of 0-25°N, 65-110°E, daily composite maps have been created. These maps were examined in order to confirm the results acquired from sodar.

3 Storm History

According to the Indian Meteorological Department (IMD), a low pressure region emerged over the Eastern Arabian Sea on 31st May, 2020, and remained a well-marked low pressure area till the evening. It became a depression over the East-Central and South-East Arabian Sea in the early morning of 1st June. It later worsened into a profound depression on the same day (DD). Around noon on 2nd June, the DD became a cyclonic storm and was given the name Nisarga. It then became an Extreme Cyclonic Storm (SCS) with a peak wind speed of 110 kmph, and a tropical cyclone with a mean wind speed of 140 kmph. Nisarga was dropped near the town of Alibag at 12:30 IST (07:00 UTC) on 3rd June, 2020, at peak strength. In nearby Ratnagiri, the peak wind speed was 110 km/h (70 mph), with a minimum pressure of 984 hPa. Figure 2

shows an IMD satellite photo of the Nisarga storm coming through Alibagh on India's western coast (website of IMD, www.imd.gov.in). The anticyclonic circulation in the middle and upper troposphere levels northeast of the system centre was primarily responsible for the storm's clockwise recurving trajectory.

4 Observed Signature Of Nisarg Cyclone

Figure 3 illustrates the vector plot of wind for height 40 to 1000 m having moderate wind speed of 10 m/s for the period 31st May to 05th June 2020. This figure indicates that the day before and after the cyclone was predominated by the southwesterly wind. Because of the interference from the neighbouring topography at the observational site, the wind profiles were not stationary, but changed abruptly. In the height range of 400-600 m on 31st May wind flows from east to west, on 1st June 2020 it was north-west, on 2nd June it was westward in the direction, on 3rd June it was southeast, on 4th June and 5th June it is again flowing in the westward direction. During the night, there were calm breezes, but during the day, there were strong winds. The eastward movement of moisture across the Indian Ocean and southeast of the BoB region increasingly accelerated as the day progressed. Over the regions, eastward moisture was continually spinning around the storm. As a result of the increased moisture connected with the system, a moisture conveyor belt (MCB) formed over the region. This shows that a large-scale movement of moisture from the ocean into the cyclonic system's interior region via MCB increased the TC's severity (Routray et al. **2020**). The formation of MCB plays an active role in bringing moisture from distant oceans into the inner core of the system, resulting in enhanced latent heating and storm intensification. The storm's continued intensity leads to the creation of MCB. The LHF (Surface turbulent latent heat flux) is well known for its importance in the TC's formation and intensification.

4.1 Hourly Mean wind profiles

The hourly average wind speed and wind direction measured for the period from 31st May to 5th June 2020 over Atigre, Kolhapur is shown in figure 4 (a-f). On 31st May, 2020 from 0000 IST to 0600 IST wind flow in a southwest direction with wind speed in the range of 9 to 13 m/s, while during 0600 IST to 1800 IST wind speed decreases from 13 m/s to 9 m/s. In the night time on that day wind flows in the same direction, but wind speed decreases at about 4 m/s. On 1st June 2020 it is observed that from 0000 IST to 0600 IST wind flow with very less speed ranging from 5 to 10 m/s in east west direction. As the solar radiations start to come then wind speed initially increases from 10 m/s to 14 m/s. It is because the depression starts early in the morning of 1st June. On that day, maximum wind speed of 14 m/s is observed at 1400 IST and afterwards decreases to 8 m/s at 1800 IST. From 1800 IST onwards in the night wind decreases to 4 m/s. It signifies that calm winds persisted at night and breezy conditions prevailed during the day. Local atmospheric circulations can be caused by the temperature differential between water and land, which can alter winds. Because the Earth's surface cools considerably more quickly than the air above it at night, wind speed tends to decrease after sunset. Winds will blow day or night if there is a low pressure system or storm in the vicinity. The highest surface cooling can occur on a quiet night.

On 2nd June early in the morning depression intensified into deep depression and hence from 0000 IST-0600 IST wind flows from east to westward direction with a speed of 8 m/s to 15 m/s. After 0600 IST deep depressions start to intensify and results into severe cyclonic storm hence wind speed becomes maximum from 0600 IST - 2400 IST. Maximum wind speed occurs on that day is 17 m/s. Warmer air is blended downward to the surface on a windy night, preventing temperatures from plummeting as quickly as they would on a clear night. As a result, a windy night will have somewhat warmer temperatures than a calm night.

On 3rd June at 1230 IST cyclone was dropped near the town of Alibag. On that day also cyclone effect is observed on the wind speed. The average wind speed was 17 m/s during day and night time as well and wind flows in the southward direction. On 4th and 5th June at 0000 IST to 0600 IST wind flow with a speed of 12 m/s. Above 0600 IST to 1800 IST maximum wind speed of 16 m/s is observed. At 1800 IST onwards wind speed start to decrease and becomes calm wind at night time and follows the normal behaviour. In this case wind direction is south to the west, which usually observes during monsoon time over Arabian sea.

Generally, in the early morning wind speed start to increase and it decrease in the night time and wind flows mainly westerly to south-westerly except on the deep depressing day and cyclone day i.e., on 2nd and 3rd June 2020. On 2nd and 3rd June wind changes its direction and becomes south-easterly. From the discussion, it is clear that with the cyclone the wind speed and its direction changed and reversed.

4.2 Vertical wind pattern

Figure 5 (a-f) shows the variation of wind vector during 31st May to 05th June 2020. The measurement was taken from the height of 40-980 m from the surface. The flow of usual monsoon mean wind flow is southwesterly on 31st May whereas on 1st June from 0000 IST-0400 IST wind flows in a southwest direction and after 0400 IST-1500 IST, direction of the wind was northeast. Afterwords it become southeasterly. On 2nd June prior to cyclone wind direction was east-south up to 0600 IST on 3rd June but after 0600 IST wind direction shifts vertically and become south-west. On 3rd June i.e. on event day wind accelerates and the maximum acceleration is noticed a wind flows in east-south and south-west direction. After the event, i.e. on 04th June and 05th June 2020 direction become southwesterly. The intense down mixing of momentum from upper levels due to solar heating causes the surface winds to intensify during the day (Sandeep et al. **2014**). Radiative (nocturnal) cooling in the boundary layer during the night reduces eddy viscosity and momentum transfer from upper levels, lowering wind speed (Mohan et al. **2016**).

Figure 6 depicts changes in atmospheric parameters such as wind speed, direction, air pressure, relative humidity, and rainfall during a tropical cyclone. Figure 6 shows how wind speed reaches a maximum of 12 m/s during a severe tropical cyclone (a). The wind speed is presented on several days, and it has been observed that the wind speed increases as the cyclone intensifies and then returns to normal after the cyclone. It is obvious from this that the maximum wind speed on the 3rd of June 2020, i.e. during the time of the cyclone, was 12 m/s. These results are well agreed with wind speed recorded in the figure 4.

Figure 6 (b) illustrates the wind direction during occurrence of the cyclone. On 31st May, 2020 we observed normal wind flow. Further wind direction changes from south-west to easterly on 1st June which shows the initiation of the cyclone. On 2nd June the direction of wind changes and it flows from south-east. On the 3rd June, after 12:00 (IST), change in the wind direction from the southeast to the south-west is observed, which is also observed from the Sodar data. Figure 6 (c) shows observed atmospheric temperature over Atigre region. Before cyclone the temperature was more comparable to the temperature after cyclone. The maximum atmospheric temperature is observed on 31st May, further change is observed during the period of 1st to 3rd June where the temperature decreases and the minimum temperature is observed on 3rd June 2020. Afterwards it again follows the same increasing trend. In the region, behind this the heat reflection in the normal time at ground is higher. Inverse variation is observed in case of atmospheric pressure and relative humidity as shown in the figure (d) and (e). The region behind this the heat reflection reduces the humidity.

Figure 7 depicts the daily mean vertical profile of wind speed from a height of 40-980 metres between 31st May and 5th June, 2020. Before and after the event, wind speeds were recorded as low as 4 m/s and as high as 8 m/s, with the maximum recorded on 3rd June, 2020, the event day. Below 700 metres above the earth, it is obvious that as height increases, wind speed increases as well, with day-to-day variance. Above that, the nature of mixing may be seen. As the wind speed rises, so does the cyclone's strength, as well as its destructive potential.

4.3 Vertical Structure of the Wind Field

Figure 8 shows wind rise plots for wind speed and direction from Sodar observations for the period from 31st May to 5th June, 2020. During the event, wind rose plots were constructed for both day and night hours. The distribution of wind speed did not change greatly with height, but the distribution of wind directions changed in a regular way. At all altitudes, south-north winds were uncommon. It has been found that as height increases, wind speed increases due to a reduction in the amount of barriers present. On the 1st and 2nd of June, the wind direction changes. During the Cyclone on the 2nd and 3rd of June, the greatest wind speed is recorded. Since the 4th of June, the wind has been blowing from the south-west, with a lower wind speed. As demonstrated in Figure 6, these results are in good agreement with AWS results.

4.4 Vertical Turbulence Pattern

The vertical turbulence intensity components (σ_w) are important for atmospheric stability characterization. The profile of σ_w observed before and after cyclone is shown in the figure 9. An increase in σ_w with height is observed at the height of 75 m and is constant in the range between 75 and 240 m layer, but the effect of the cyclone on 3rd June, 2020 has shown an increase in the turbulence.

5 Era5 Reanalysis

5.1 Atmospheric Pressure

Figure 10 (a-f) depicts the mean sea level pressure distribution and shows how these systems quickly transitioned from cyclonic storms to very severe cyclonic storms as they approached the shore from 1st to 3rd June, 2020. The Nisarg cyclone's core pressure ranged from 1000 to 1008 hPa, with the lowest value observed when the cyclone became a very severe cyclonic storm on 2nd and 3rd June, 2020, at 16°N, 72°E and 18.5°N, 72.5°E, respectively. The low value (1000 hPa) corresponds to the days of 2nd and 3rd June, 2020, when the system was transitioning from a cyclone to a severe cyclonic storm. The cyclone's progressive intensification was indicated by falling pressure to the left of the track. The central pressure of the deep depression on 1st June, 2020, at 14.8°N, 71.5°E, was 1008 hPa, somewhat higher than the strong cyclonic storm on 2nd June, 2020, at 14.8°N, 71.5°E.

5.2 Wind field

Figure 11 (a-f) shows the daily mean time series wind speed and direction. The wind speed varied between 3-15 m/s in the Arabian sea and it increased on 2nd and 3rd June, 2020 before landfall. From the figure (a) it is clearly observed that an elongated cyclonic circulation with strong wind (3-9 m/s) over the southwest sector of the storm. The magnitude and structure of wind pattern are reasonably well matched with the sodar analysis. In general, the southwest (SW) sector of the storm has higher winds during the pregenesis stage than the other sectors [northeast (NE), northwest (NW), and southeast (SE), and the amplitude of the wind in the SW sector gradually decreases as the storm intensifies. In comparison to the 31st May forecast, the system expanded further on 1st June (see figure b), with the wind magnitude increasing over a vast area. On the 1st of June forecast, the cyclonic circulation is more evident. However, forecasts for the 2nd and 3rd of June (figures c and d) suggest a more powerful cyclonic storm with strong winds of 3 to 15 m/s. After landfall on the 4th and 5th of June 2020, the wind circulation shifts from west to east, with wind speeds ranging from 3 to 9 m/s. According to the IMD data, the storm progressed from depression to cyclonic storm phases from 31st May to 5th June, 2020.

5.3 SST and OLR

Figure 12 depicts the SST and OLR composite from 31st May to 5th June, 2020. As a proxy for precipitation, OLR is utilised to find areas of deep tropical convection (King and Jakob **2020**). The convective area is thought to be represented by OLR values below 240 Wm^{-2} (Mahakur et al. **2013**). OLR ranged from 100 to 240 Wm^{-2} in the active convective zone along Nisarg's track (12°-18.5°N, 72.5°-75°E). Low levels of OLR varied between >100-160 Wm^{-2} were co-located with warmer SST (30-31°C) in the Arabian sea during the cyclone's active days, as illustrated in figures (c-e). When Nisarg approached India's south coast, the dramatic drop in OLR values suggested increased convective activity. OLR values climbed to 240-280 Wm^{-2} after impact on June 4th .

5.4 Vertical Wind Shear

The Vertical Wind Shear (VWS) field between 200 and 850 hPa levels was shown in figure 13 (a-f) from 31st May to 5th June, 2020. The VWS is a key dynamical component that influences the strength and pattern of tropical cyclones (Jinhua Yu et al. **2010**). The VWS has long been known to have a significant impact on tropical storm development, structure, and intensity (Zhang and Tao et al. **2013**). When VWS is low, the genesis of a system is accelerated, whereas when it is high, the genesis is slowed. Low VWS values were found to the north of Nisarg's track, indicating the presence of favourable circumstances for the cyclone to persist for a longer length of time.

6 Discussion

The tropical cyclone 'Nisarg,' which hit India's west coast during the pre-monsoon season, formed in the Eastern Arabian Sea. It moves from a low pressure area over the eastern Arabian Sea to Alibagh (18.60°N, 72.87°E) on the western coast of India on 3rd June, 2020. On the 2nd and 3rd of June 2020, the lowest atmospheric pressure of 1000 hPa was recorded at nearby Ratnagiri (16.99°N, 73.31°E), with the maximum wind speed of 110 km/h (70 mph). Wind speeds at the Sodar location (Atigre) ranged from 4 to 17 m/s during 31st May to 5th June, 2020. The wind speed before and after the cyclone was 4-8 m/s, with a maximum wind speed of 17 m/s on 3rd June, 2020. Wind direction changes dramatically from 0 to 360° in an oscillating pattern. The wind direction during this time was south-west on the 31st of May, then east-west on the 1st and 2nd of June. After the cyclone made landfall on 3rd June, the wind shifted back to the south-west on 3rd June, 2020.

When the aforesaid meteorological conditions in the current study were compared to those reported, there was a striking similarity. Before the storm crossed the observational location (Gadanaki) on 21st June, 2007, (Kumar et al. **2014**) noted severe westerly winds >10 m/s. It is observed that as it crosses the shore on 22nd June, 2007, the wind direction shifts to easterly throughout the ABL. The wind direction in Large Typhoon T9426 shifted from north to west, counterclockwise. Small Typhoon T9503 had a clockwise shift in wind direction from east to south (Amano et al. **1999**). The response of the Bay of Bengal to the super cyclones Gopalpur and Paradip between 15th and 31st October 1999 was investigated (Chintalu et al. **1999**). As the storm intensifies, they noticed changes in meteorological parameters such sea surface temperature (SST), air temperature (Ta), wind speed (Ws), wind direction (Wd), and ocean currents (Cs). They saw a significant increase in wind speed to 5.8 m/s, as well as an abrupt change in direction from 30° to 270° clockwise, which remained approximately 270° to the north. In order to comprehend the prominent causes of the Andhra Pradesh cyclonic storm in the Bay of Bengal in September 1997, (Chintalu et al. **2012**) researched the salient features of the storm. The wind direction has radically shifted from 0° to 360° in an oscillating fashion, which is a crucial trait during the period of incipient development, according to this study.

The effect of the storm on the current wind speed and direction has been clearly revealed by these remote observations. The lowest value of atmospheric pressure of 1000 hPa was observed in the ERA5 reanalysis during the 2nd and 3rd June 2020. In the latitude range of 16–18.5°N, 72–72.5°E, the SST was cooler to the right of the cyclone track than to the left. SSTs were found to be higher to the left of the

cyclone track. The wind speed ranged from 3 to 15 m/s. The wind field in the Arabian Sea showed notable cyclonic circulation from 1st to 4th June, 2020, and strengthened on 2nd and 3rd June before reaching landfall on the Alibag coast. The low values of OLR were co-located with warmer SST in the Arabian Sea during cyclonic activity days from 2nd and 3rd June 2020. As the storm reached India's west coast, the OLR dropped, indicating increased convective activity.

7 Conclusion

Initial results of newly installed the Phased Array Doppler Sound Detection and Ranging (SODAR) at the Center for Space and Atmospheric Science (CSAS), Sanjay Ghodawat University, Kolhapur (16.74° N, 74.37° E; near India's western coast) by Indian Institute of Tropical Meteorology, Pune are presented.

The observations of the Nisarg Tropical Cyclone are the first of their sort at Atigre. We found that drastic change in speed and direction of wind, temperature, relative humidity and atmospheric pressure below 700 metres altitude during 14:00 IST on 02 June 2020 to 12:00 IST on 3rd June, 2020 in the measurements of Sodar and AWS.

The results presented in this study illustrates the unique qualities of this tropical cyclone movement, which may aid in the study and improvement of forecasting such systems, as well as disaster management's ability to limit losses caused by tropical storm natural hazards.

The cyclones that originate in the Arabian Sea traverse India's west coast after making landfall.

Declarations

Acknowledgement

The authors gratefully acknowledge to the Director, Indian Institute of Tropical Meteorology, Pune for his support and encouragement in providing necessary facilities and observations to carry out this work. The authors are thankful to the Indian Meteorological Department (IMD), Pune for providing AWS data. We are grateful to the Vice Chancellor of Sanjay Ghodawat University, Kolhapur for his support and the Principal, Bharati Vidyapeeth's Dr. Patangrao Kadam Mahavidyalaya, Sangli for constant encouragement. All authors acknowledge the funding support of the Ministry of Earth Science (MoES), New Delhi, Govt of India.

References

1. Nair AG, Annadurai R (2018) A study on various tropical cyclone hits in India – through gis approach. Int J Pure and Appl Math 119: 589-595.
2. Amano T, Fukushima H, Ohkuma T, Kawaguchi A, Goto S (1999) The observation of typhoon winds in Okinawa by Doppler sodar. J Wind Eng Ind Aerodyn 83:11–20. doi:10.1016/s0167-6105(99)00057-4

3. Kumar A, Brahmanand PS, Nayak AK (2014) Management of Cyclone Disaster in Agriculture Sector in Coastal Areas. Directorate of Water Management. Bhubaneswar. P108
4. Asnani GC (2005) Tropical meteorology (Indian Insitute of Tropical Meteorology, Pune, India).
5. Bhatla R, Raj R, Mall RK, Shivani (2020) Tropical Cyclones Over the North Indian Ocean in Changing Climate. Techniques for Disaster Risk Management and Mitigation, 63–76. https://doi.org/10.1002/9781119359203.ch5
6. Chinthalu GR, Dharmaraj T, Patil MN, Dhakate AR, Pawar SD, Siingh DK (2018) Severe cyclonic storm JAL, air-sea interaction perspectives and floods along Andhra Pradesh-Tamilnadu coast. J. Indian Geophysical Union, 22:341-348.
7. Emanuael KA (1986) An air-sea interaction theory for tropical cyclones. Part –I: Steady state maintenance. J Atmos Sci 48:585-604.
8. Cheynet E, Liu S, Ong MC, Jakobsen JB, Snæbjornsson J, Gatin I (2020) The influence of terrain on the mean wind flow characteristics in a fjord. J Wind Eng Ind Aerodyn 205: 104331.
9. Giammanco IM, Schroeder JL, Powell MD (2013) GPS drop wind sonde and WSR-88D observations of tropical cyclone vertical wind profiles and their characteristics. Wea. Forecasting 28:77-99. http://dx.doi.org/10.1175/WAF-D-11-00155.1.
10. Hendricks EA, Braun SA, Vigh J L, Courtney JB (2019) A summary of research advances on tropical cyclone intensity change from 2014-2018. Tropical Cyclone Research and Review, 8: 219–225. doi:10.1016/j.tcrr.2020.01.002.
11. Murakami H, Vecchi GA, Underwood S (2017) Increasing frequency of extremely severe cyclonic storms over the Arabian Sea. Nature Climate Change, 7:12, 885-889.
12. Yu J, Tan ZM, Wang Y (2010) Effects of Vertical Wind Shear on Intensity and Rainfall Asymmetries of Strong Tropical Storm Bilis (2006), Adv. Atmos. Sci. 27:552-561, doi:10.1007/s00376-009-9030-6.
13. Lyulyukin V, Kallistratova M, Zaitseva D, Kuznetsov D, Artamonov A, Repina I, Petenko I, Kouznetsov R, Pashkin A (2019) Sodar Observation of the ABL Structure and Waves over the Black Sea Offshore Site Atmosphere 10:811. https://doi.org/10.3390/atmos10120811.
14. Kallistratova M, Coulter R (2004) Application of sodar in the study and monitoring of the environment, Metero. Atmos. Phys. 85: 21-37 https://doi.org/10.10,07/s00703-003-0031-1.
15. King MJ, Jakob C (2020) Rain and Cloud Perspectives on the Seasonal Cycle over the Western Equatorial Indian Ocean, J Clim 33: 925-940. https://doi.org/10.1175/JCLI-D-19-0080.1
16. Kumar MS, Anandan VK, Kesarkar A, Reddy PN (2011) Doppler SODAR observations of the temperature structure parameter during monsoon season over a tropical rural station, Gadanki. J Earth Syst Sci 120:65-72. https://doi.org/10.1007/s12040-011-0007-3
17. Lyulyukin VS, Kallistratova MA, Kouznetsov RD, Kuznetsov DD, Chunchuzov IP, Chirokova GY (2015) Internal Gravity-Shear Waves in the Atmospheric Boundary Layer by the Acoustic Remote Sensing Data. Izv. Atmos Ocean Phys 51:193–202. doi:10.7868/S0002351515020108

18. Mahakur M, Prabhu A, Sharma AK, Rao VR, Senroy S, Randhir Singh and B. N. Goswami (2013) A high-resolution outgoing longwave radiation dataset from Kalpana-1 satellite during 2004–2012, Curr Sci 105: 1124-1133.
19. Mohan T S, Rao TN (2016) Differences in the mean wind and its diurnal variation between wet and dry spells of the monsoon over southeast India. J Geophys Res Atmos 121:6993–7006. doi:10.1002/2015JD024704.
20. Nade DP, Potdar SS, Pawar RP, Taori A, Kulkarni G, Siingh D, Pawar SD (2020) Intra-annual variations of regional total column ozone, aerosol optical depth, and water vapor from ground-based, satellite-based and model-based observations. Atmos Res 237: 104860. https://doi.org/10.1016/j.atmos.res.2020.104860.
21. Niranjan Kumar K, Rao CK, Sandeep A, Rao TN (2014) SODAR observations of inertia-gravity waves in the atmospheric boundary layer during the passage of tropical cyclone. Atmos Sci Let 15: 120–126. http://dx.doi.org/10.1002/asl2.478.
22. Obasi, GOP (1977) WMO's programme on the tropical cyclone, Mausam. 48:103-112.
23. Pattanayak S, Mohanty UC (2008) A comparative study on performance of MM5 and WRF models in simulation of tropical over Indian seas. Curr Sci 95:923-936.
24. Raju PVS, Potty J, Mohanty U C (2011) Sensitivity of physical parameterizations on prediction of tropical cyclone Nargis over the Bay of Bengal using WRF model, Meteorol Atmos Phys 113:125–137. doi:10.1007/s00703-011-0151-y.
25. Reddy MV, Surendra Prasad SB, Murali Krishna UV, Reddy KK (2014) Effect of cumulus and microphysical parameterizations on the JAL cyclone prediction. Indian J Radio Space Phys 43:103-123.
26. Routray A, Lodh A, Dutta D, George JP (2020) Study of an Extremely Severe Cyclonic Storm "Fani" over Bay of Bengal using regional NCUM modeling system: A case study. J Hydrol 59: 125357. https://doi.org/10.1016/j.jhydrol.2020.125357.
27. Sahoo B, Bhaskaran PK (2015) Synthesis of Tropical Cyclone Tracks in a Risk Evaluation Perspective for the East Coast of India. Aquat Procedia 4:389–396. doi:10.1016/j.aqpro.2015.02.052.
28. Sandeep A, Rao TN, Ramkiran CN, Rao SVB (2014) Differences in atmospheric boundary layer characteristics between wet and dry episodes of the Indian summer monsoon. Boundary-Layer Meteorol 153:217–236. doi: 10.1007/s10546-014-9945-z
29. Stramma L, Cornillon P, Price JF, (1986) Satellite observations of sea surface cooling by cyclones. J Geophys Res 91 C4 5031-5035.
30. Tse KT, Li SW, Chan PW, Mok HY, Weerasuriya AU (2013) Wind profile observations in tropical cyclone events using wind-profilers and Doppler SODARs, J. Wind Eng. Ind. Aerodyn.115: 93–103. https://doi.org/10.1016/j.jweia.2013.01.003
31. Zaitseva DV, Kallistratova MA, Lyulyukin VS, Kouznetsov RD, Kuznetsov DD (2018) The Effect of Internal Gravity Waves on Fluctuations in Meteorological Parameters of the Atmospheric Boundary Layer. Izv. Atmos. Ocean. Phys. 54, 173–181 doi: https://doi.org/10.1134/S0001433818020160

32. Zhang F, Tao D (2013) Effects of Vertical Wind Shear on the Predictability of Tropical Cyclones, J Atmos Sci 70: 975-983. doi: https://doi.org/10.1175/JAS-D-12-0133.1

Figures

Figure 1

Experimental setup of the Phased Array Doppler Sodar system with enclosure at Atigre, Kolhapur

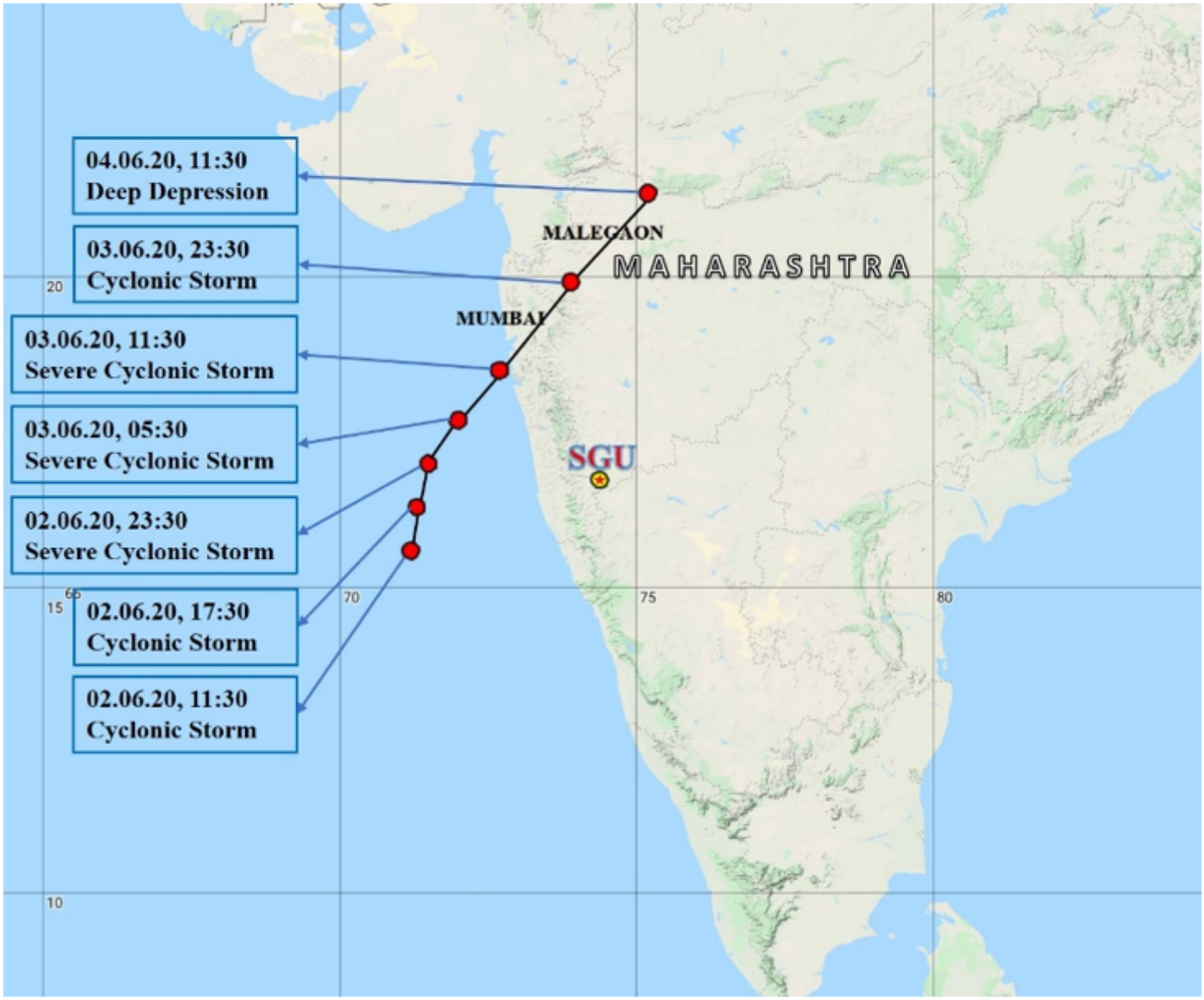

Figure 2

Track of Nisarga cyclone passed through Alibagh in the west coast of India

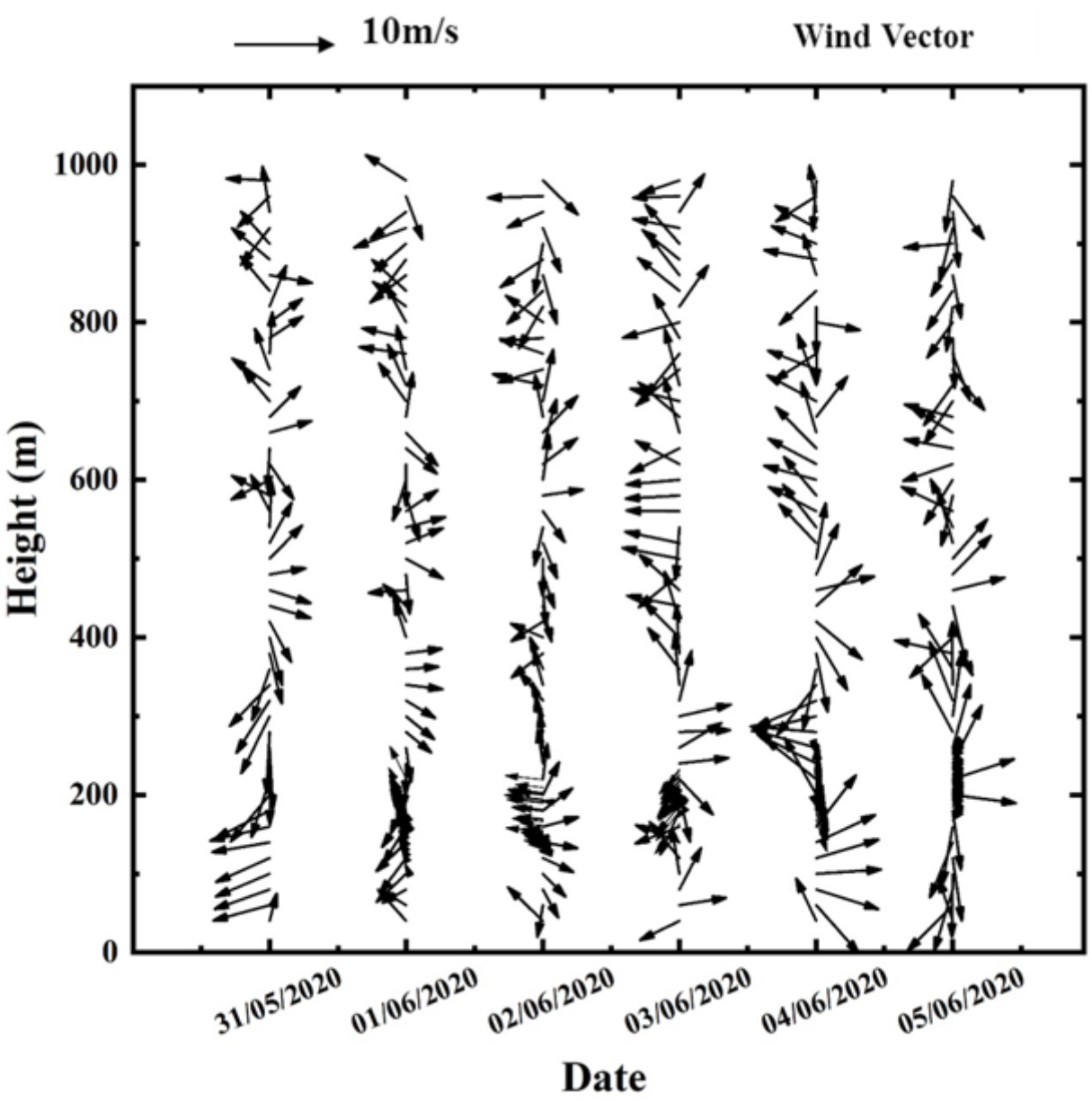

Figure 3

Wind vector plot observation during the period of 31st May to 05th June, 2020

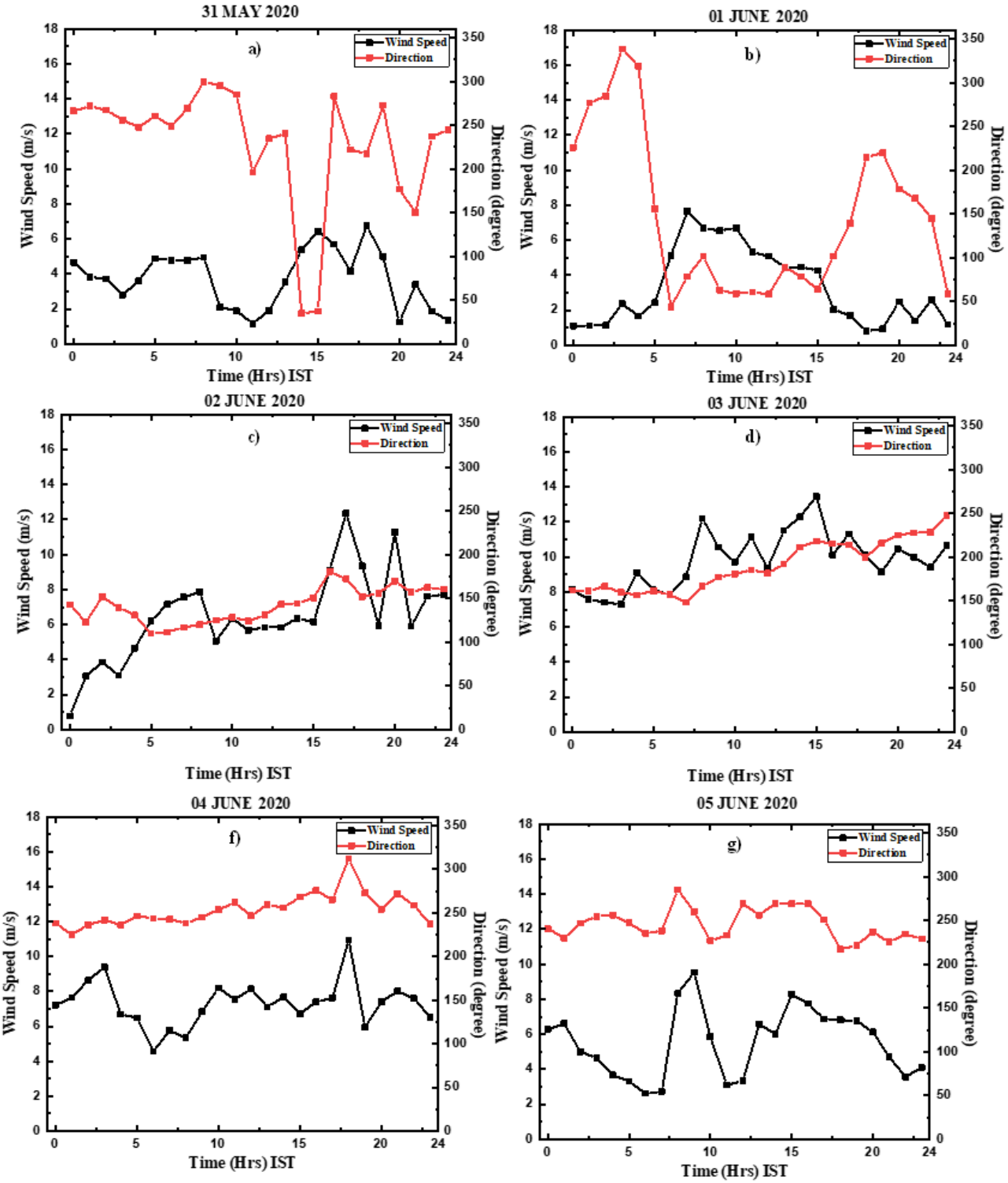

Figure 4

Variation of wind speed and direction during the period from 31st May to 05th June, 2020 at Atigre, Kolhapur

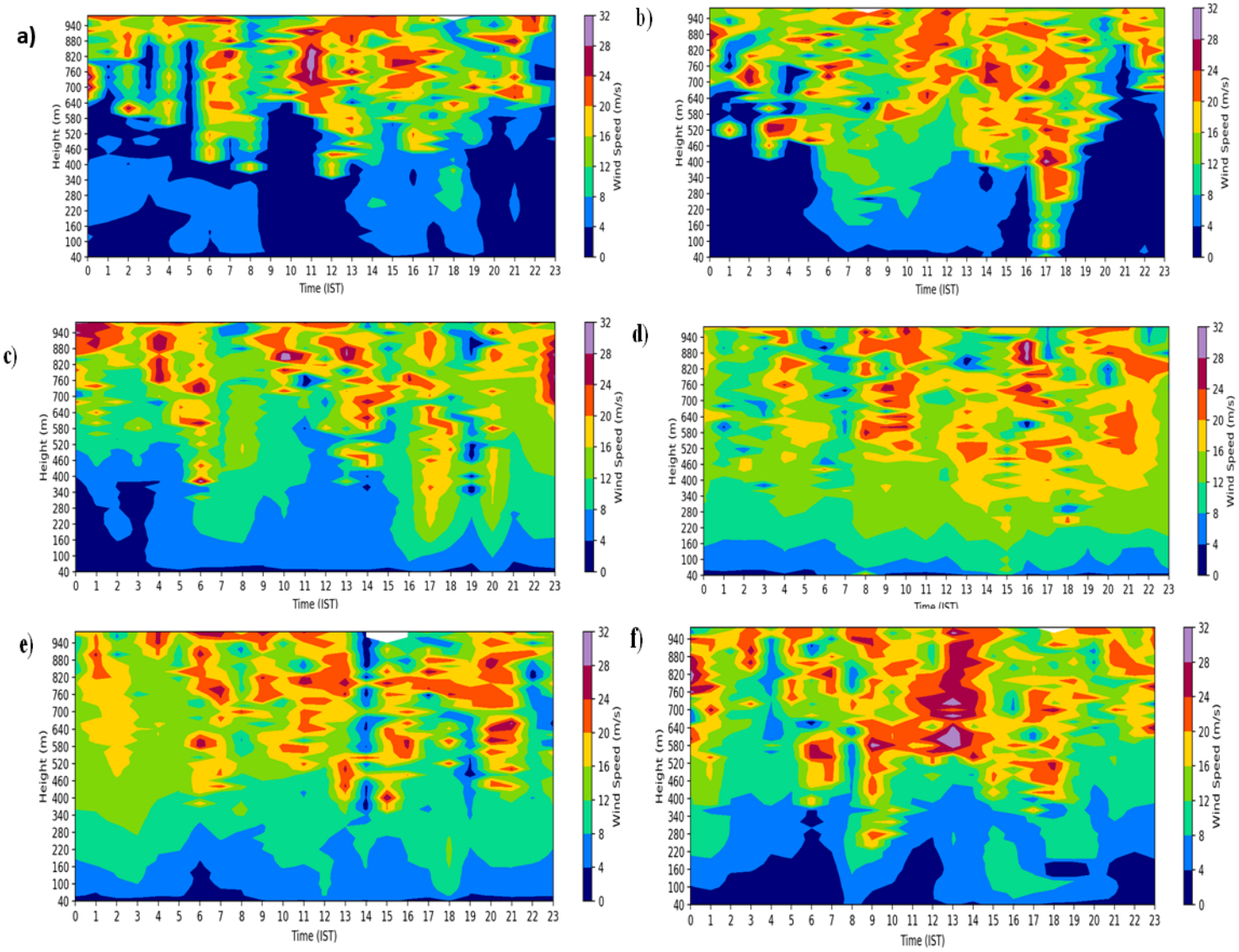

Figure 5

Time-height variation of wind vectors for 31st May, 1st to 5th June, 2020.

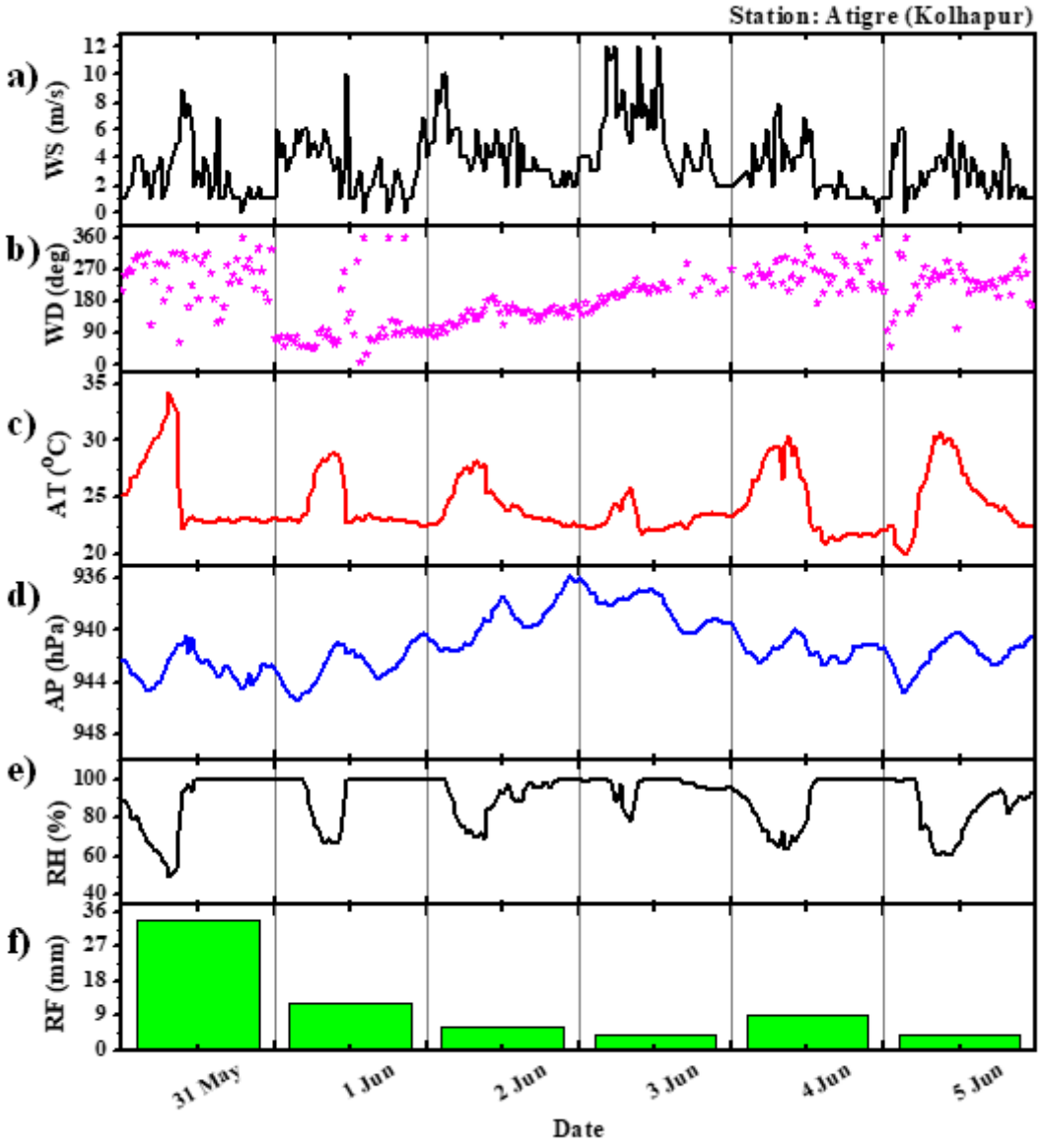

Figure 6

Atmospheric weather parameters' plot for the period from 31st May to 05th June 2020

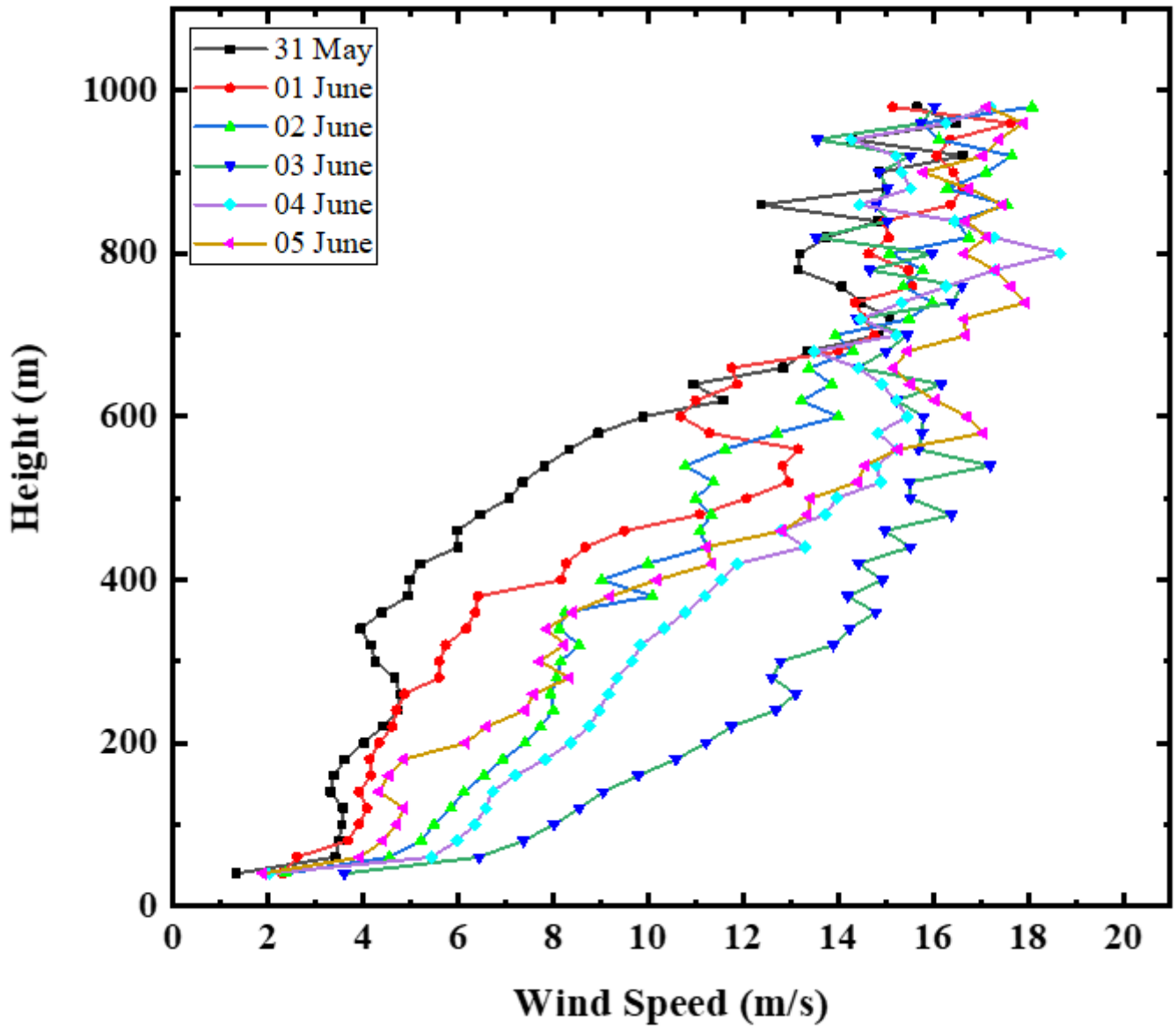

Figure 7

Vertical Wind Speed Profile on 31st May – 05th June 2020

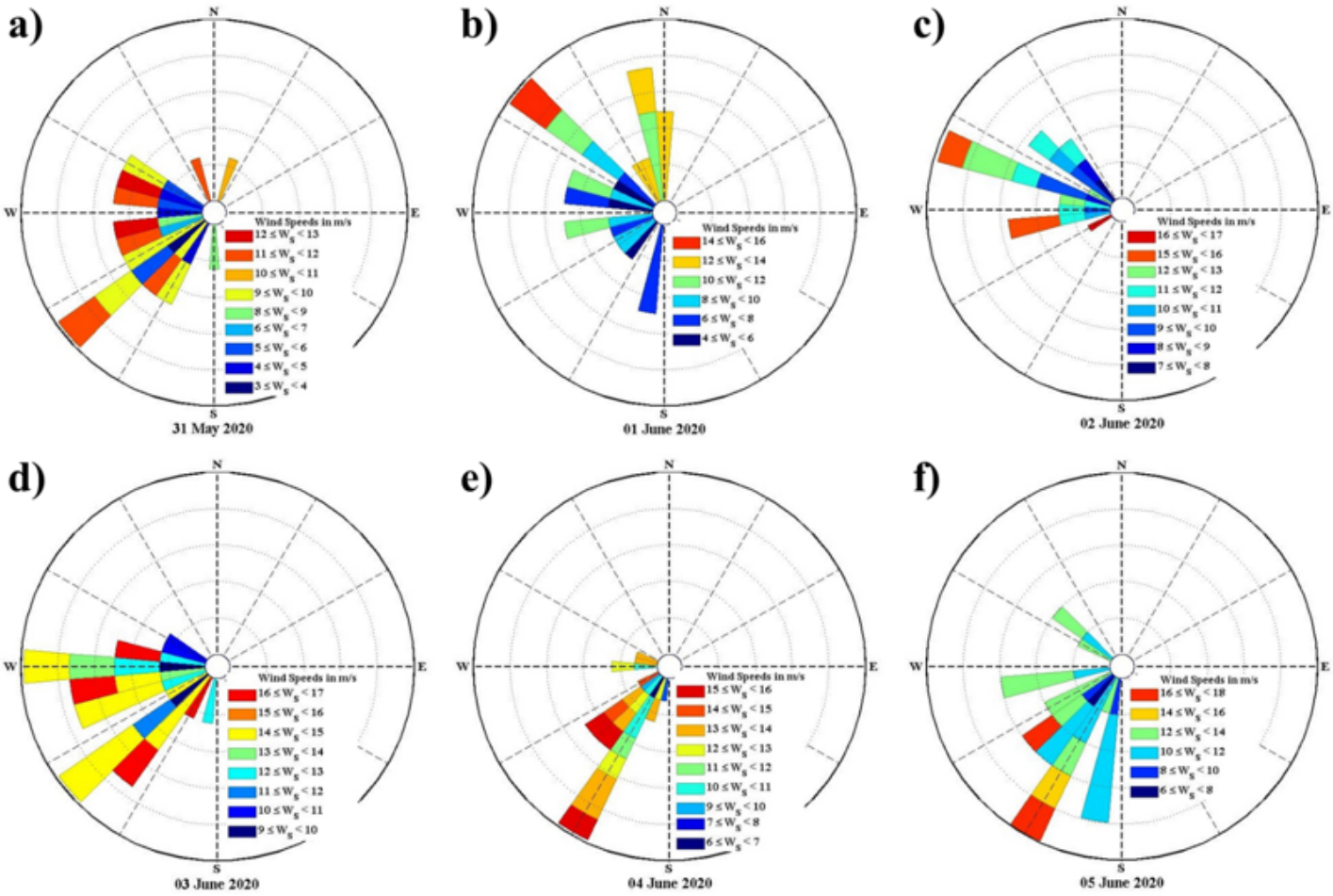

Figure 8

Height wise variation (40-980 m) of wind speed and direction from sodar measurements for 31st May – 05th June, 2020.

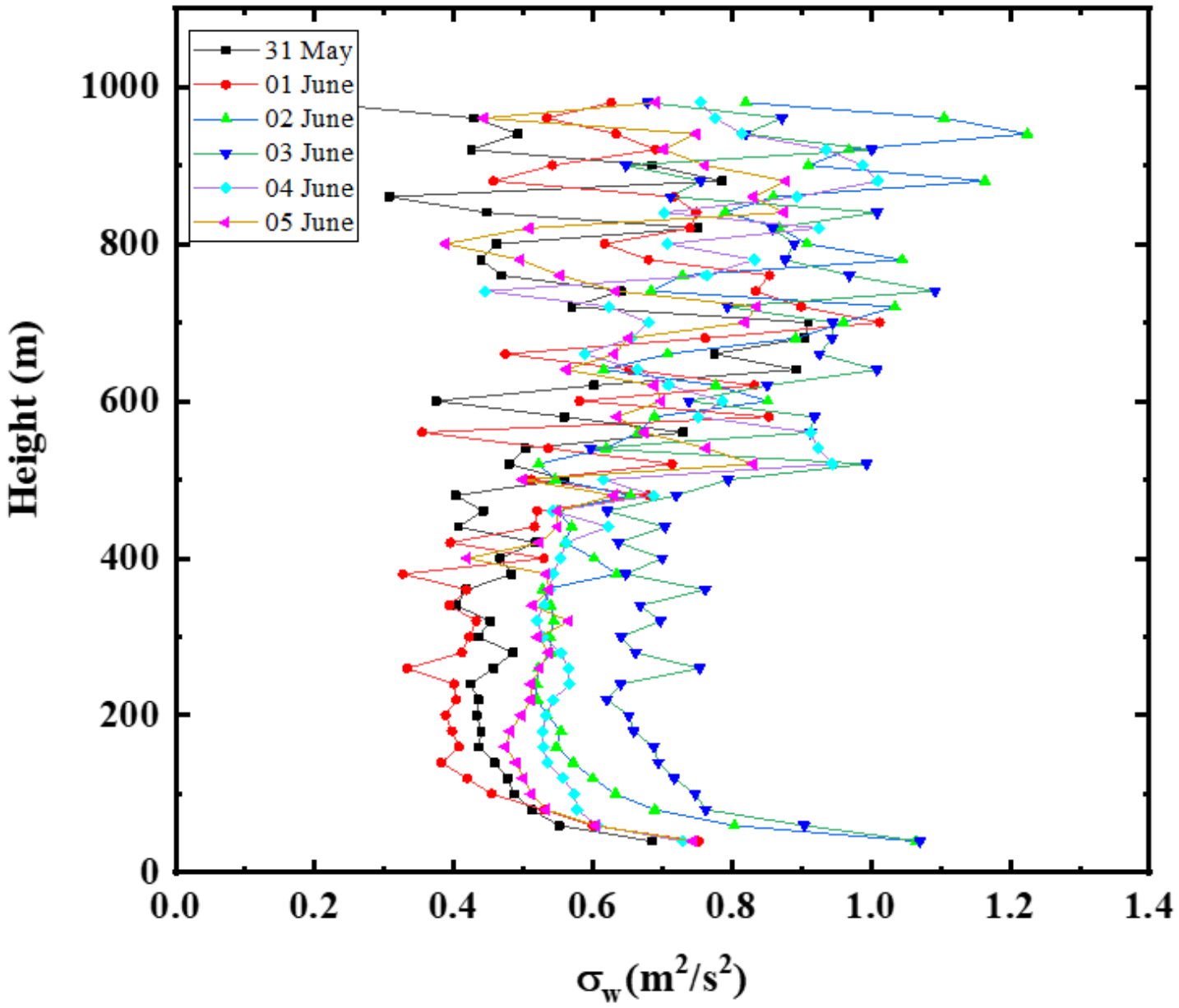

Figure 9

Variation of vertical velocity variance (σw) with height before, during and after Nisarg cyclone passage at Atigre, Kolhapur

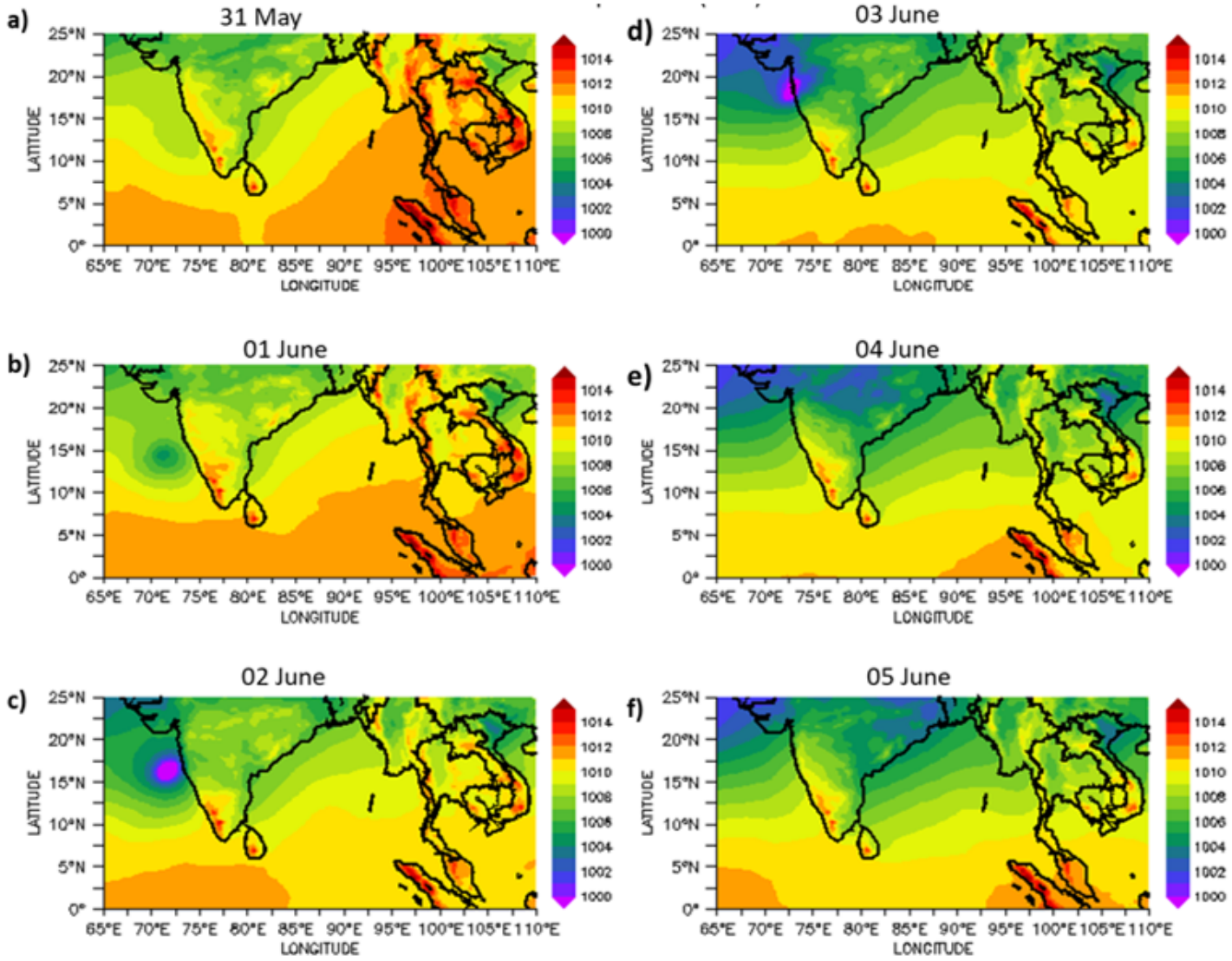

Figure 10

Daily mean sea level pressure (hPa) distribution during the period 31st May to 5th June, 2020

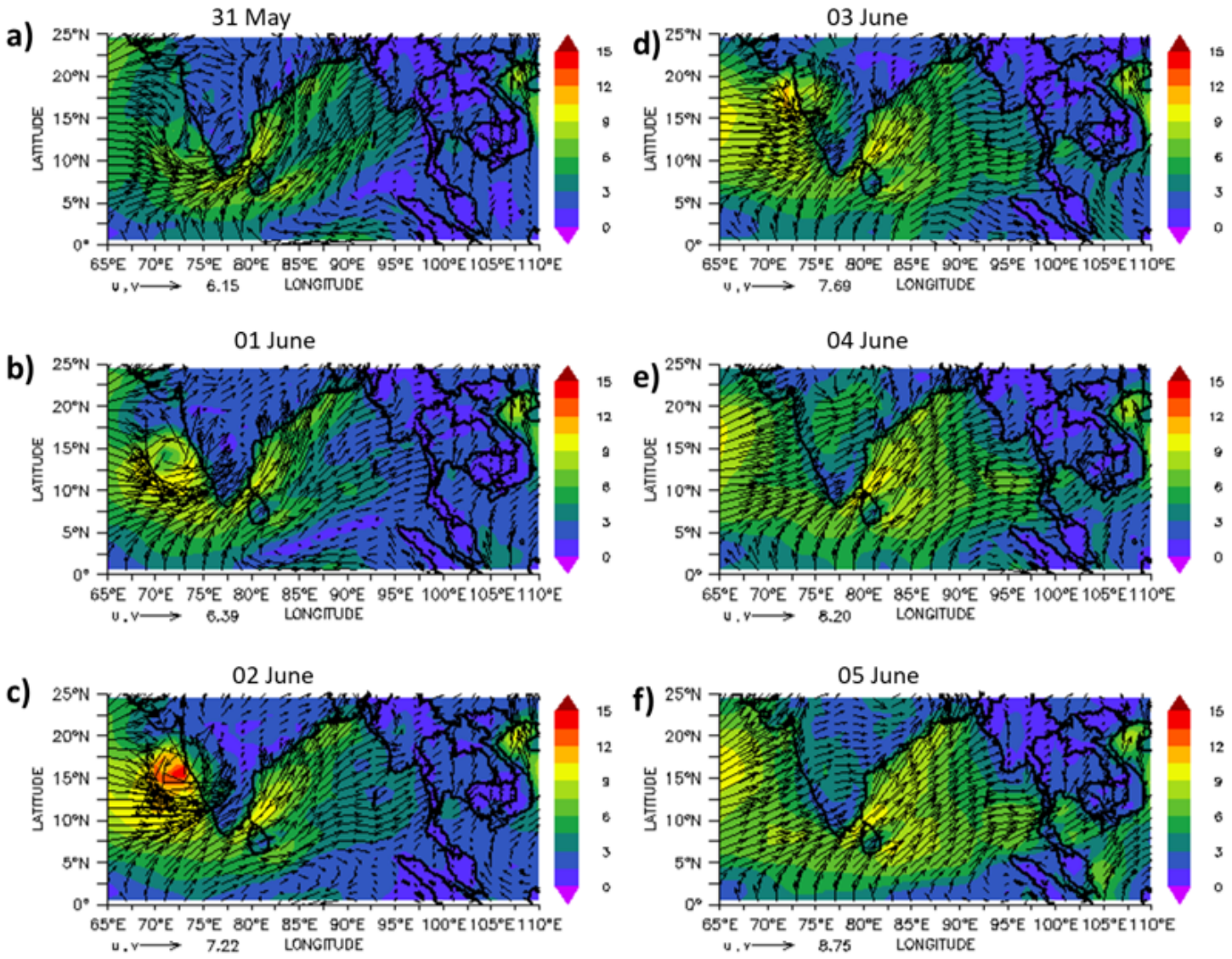

Figure 11

Wind vector and magnitude (shaded; m/s) at 850 hPa from ERA-5 reanalyses during the period 31st May to 5th June, 2020.

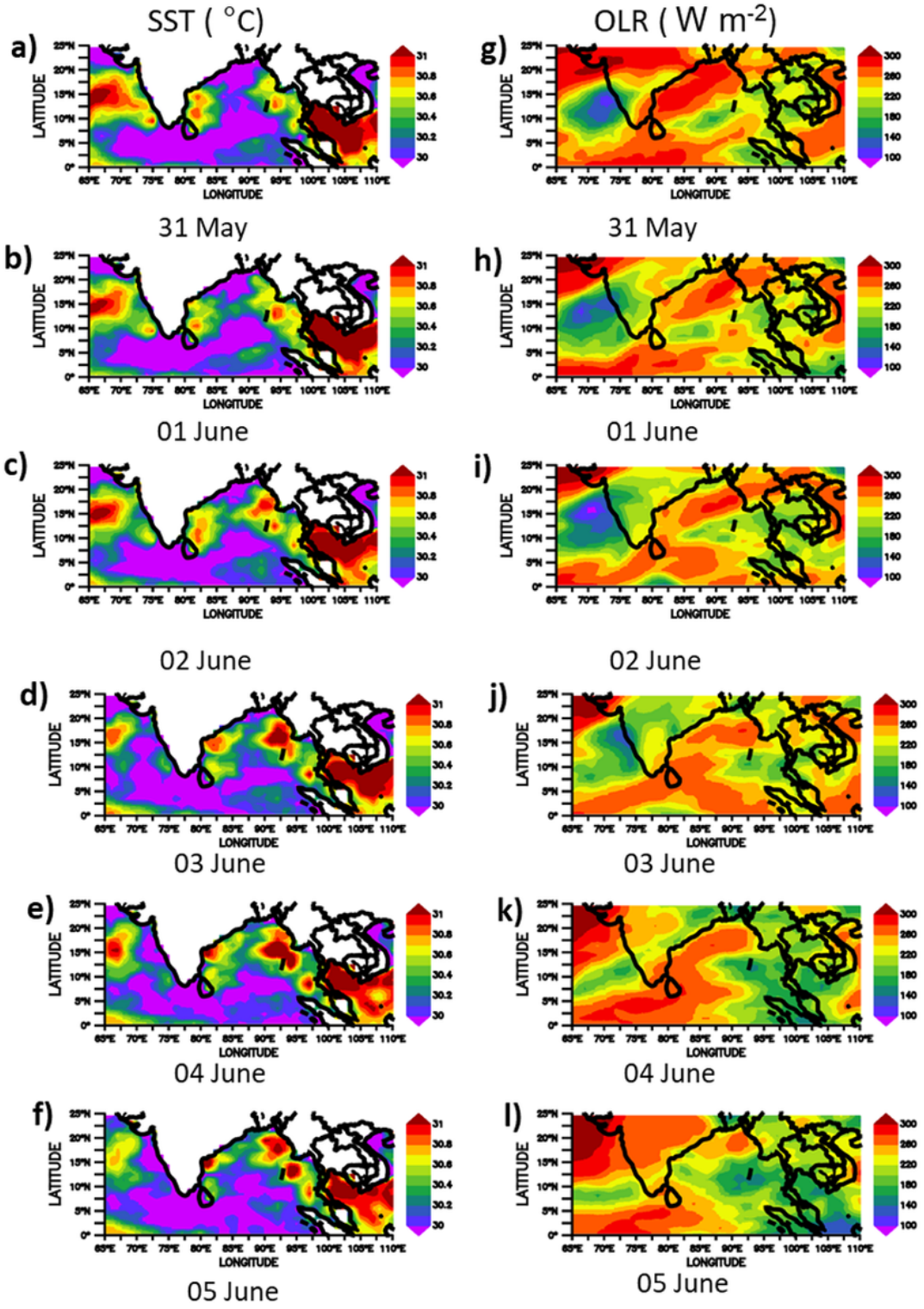

Figure 12

Daily mean of SST and OLR.

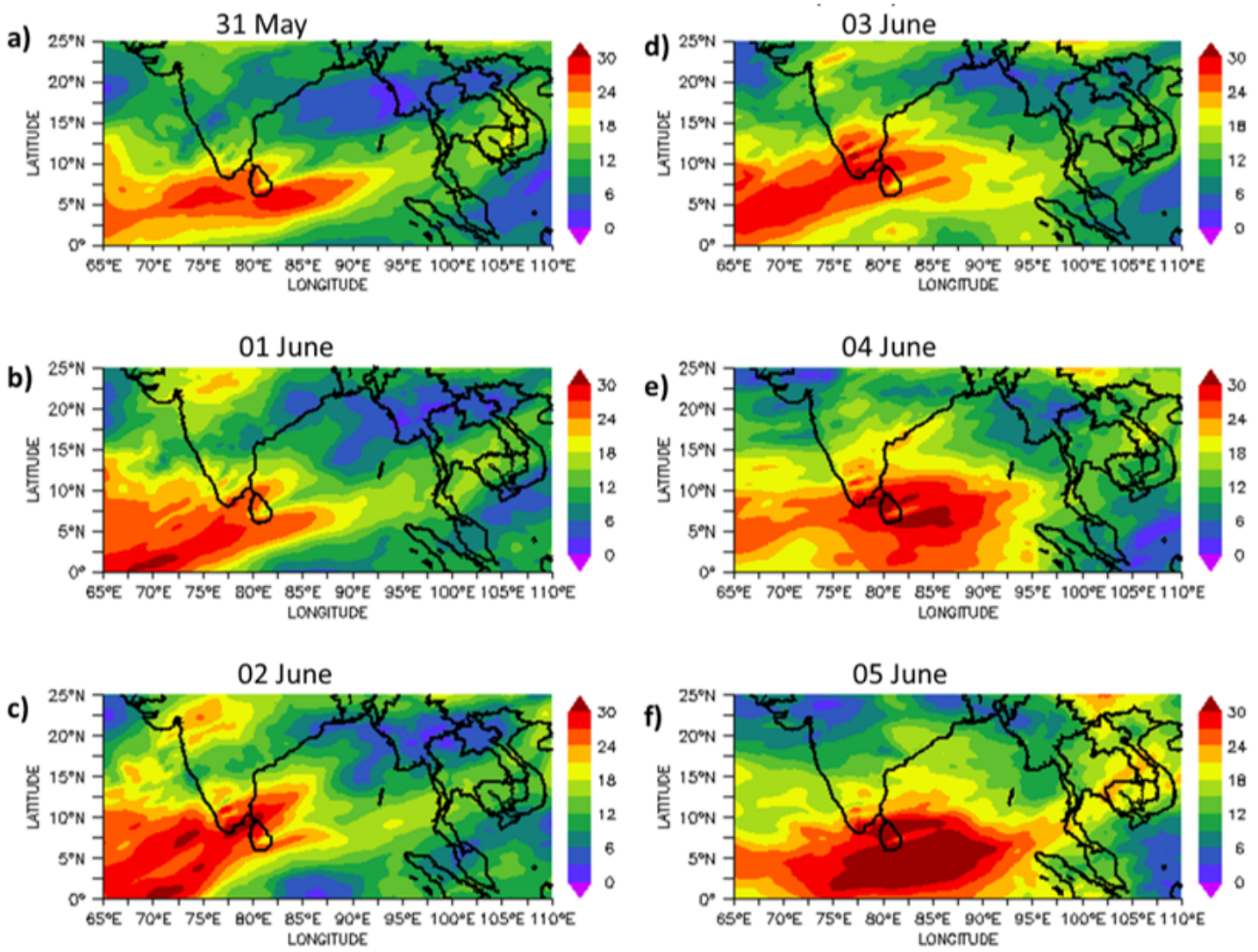

Figure 13

Vertical wind shear during the period 31st May to 5th June, 2020